Plumbing the Pudding Model of the Atom

By Eric Stanley Reiter, July 9, 2026, Pacifica CA. http://www.thresholdmodel.com. email reiter@thresholdmodel.com

Overview

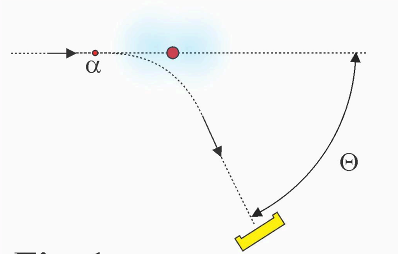

Fig. 1. Nuclear model

We will explore in this sequence: **1)** the experimental evidence initiating the nuclear model, **2)** ER's (author) experimental repeat, **3)** threshold model vs quantization, **4)** ER's past experiments with gamma γ and alpha α rays, **5)** ER's recent tests splitting the α upon a crystal surface, and **6)** conclusion. In addition to a serious challenge to quantization, this report reveals how so-called nucleons can diffract. We know of experiments that show what appears to be nucleon interference (1, 2). If you do not think this is a problem, please read up on the measurement problem. The short answer to this problem is: if it diffracts, it is a wave. We explain particle-like effects as thresholds.

1) First test of the nuclear model

An older atomic model depicts a massive positive charge extending to the size of its negative electronic influence. It is affectionately called *plum pudding*, a model proposed (not named) by JJ Thomson (3).

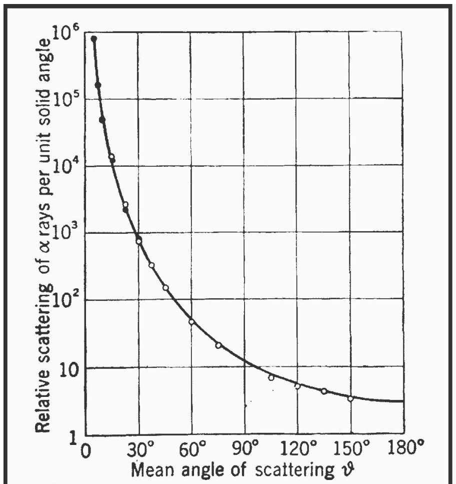

Fig. 2 α scatter from gold foil.
Data from Geiger and Marsden 1913.
Plot from Evans, *The Atomic Nucleus*, page 18.

Rutherford's theory (4) on the scattering of alpha *particles*, Geiger and Marsden's 1913 data (5), and Bohr's use of the nuclear model (6), led physicists to accept that the atom must have a small, heavy, positively charged nucleus; see **Fig. 1**. The 1913 fit to Rutherford's Coulomb derivation, as in **Fig. 2**, seems convincing, especially at large angles. In modern practice (7), background counts at angles exceeding 30° can overwhelm the effect. Furthermore, their source emitted two alpha α of different kinetic energies $\mathcal{E}$. The theory depends on $\mathcal{E}$, and they did not have detectors with pulse-height resolution. They overcame those problems by using an extremely strong source and a filter ahead of the gold that allowed only the swiftest α to interact with their zinc sulfide scintillation viewer.

In modern practice, pulse-height resolution and choice of a discriminator setting should play a major role. In search, I have not found anyone reporting this test with pulse-height resolution, nor have I found anyone substantiating Rutherford theory at large angles (7, 8). The data of **Fig. 2** is from a table in Geiger and Marsden (5) that reported no error analysis. The graph was not in (5). Was this graph in Evans generated by Evans (9)?

2) Repeating the 1913 Geiger Marsden Rutherford test result

The α background from the steel and welds of my vacuum chamber did not interfere with my previous tests using the coincidence technique, but it was a significant problem with the singles tests here. (signal)/(noise)=(background rate)/(experimental rate)=R_{back}/R_{exp}. To lower that background, the chamber was lined with plastic tape and plastic parts. This made some compromise to the vacuum, but it stabilized near 5 x 10^{-1} torr.

The source was a collection of ^{241}Am mounted behind a collimator made of 55 glass pipettes (see **Fig. 7**). The detector is an ORTEC DIAD surface barrier with a built-in amplifier, unfortunately no longer available. The amplifier and pulse height discriminator were the ORTEC 490B and 551, respectively. The scatterer was LA brand triple-thick 24K gold leaf, stacked 20 times to become 0.0003 cm thick. It was calculated by weighing with its paper, cutting it up, then subtracting the paper weight.

For each reported angle, data was collected on a Lecroy LT624 digital oscilloscope with histogram software. Data for scatterer angle Θ=90° is shown in **Fig. 3**. Analog pulse heights are plotted in histogram A and copied but shifted to the right onto trace B. Larger pulse counts are read from totp(A) in red, and the shifted pulses are counted at totp(B) in blue. dur(A) gives the time required to calculate the rates R_{BIG} and R_{ROI}.

At trace D are pulse heights from a previous test at Θ=0° through the gold. The angle of incidence to the gold in both cases was Φ=30°. Here we see the importance of choosing which pulse heights are recorded as a function of angle. The shapes of traces D to A differ greatly. The change was gradual over angle changes. If one chooses the region of interest at zero degrees and continues with that Region Of Interest ROI, the count rate would change in an unfair way as a function of angle: big mistake. A downshifted part of the spectrum is more stable for counts over a wide range of angles. More α are slowed and pass the gold there. I have not found anyone looking at pulse-height spectra to choose how to count.

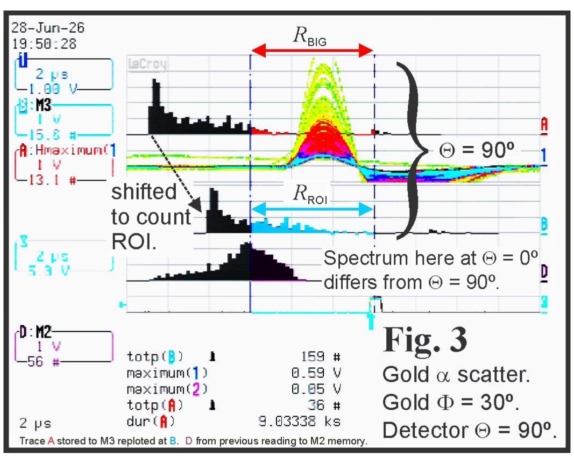

Fig. 3 Gold α scatter. Gold Φ = 30°. Detector Θ = 90°.

Fig. 4 shows my data compared to theory. **Appendix 1** is a GOOGLE SHEETS spreadsheet that outlines all the steps. A link is provided for anyone to work with my original data. Using counts in my ROI, at Θ=90°, the data drifts from theory by a factor of 2. Given my weak source, wide ΔΘ angle (see **Fig. 7**), and other possible inaccuracies, I call this good. *Melissinose's* (7) error bar was a factor of 3 larger than theory, even at 30°.

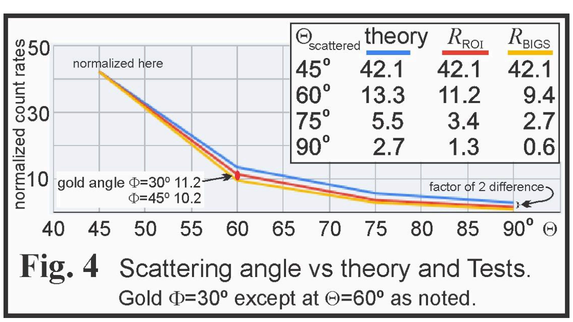

$Θ_{scattered}$	theory	R_{ROI}	R_{BIGS}
45°	42.1	42.1	42.1
60°	13.3	11.2	9.4
75°	5.5	3.4	2.7
90°	2.7	1.3	0.6

Fig. 4 Scattering angle vs theory and Tests. Gold Φ=30° except at Θ=60° as noted.

An extension of Rutherford's theory is *Rutherford Backscatter Spectroscopy*. In my search: RBS is performed only at a large fixed angle. In my search: at large angles Rutherford's equation is not obeyed at high energies. In my search: anomalies are found at large angles with some scatters, interestingly reflecting from ^{128}Si at similar MeV to ours (10). Evidently, large angle conformation to the Rutherford equation is difficult to achieve. Just how Geiger and Marsden achieved such accurate looking data is a mystery to me. The emphasis of Rutherford's original argument, and from most physicists, is that α can reflect only by a particle model. Here we show evidence that Bragg scattering can explain reflection.

3) ER's Theory in Brief

My previous work explains that past tests were not designed to distinguish quantization from a workable threshold model. My past writings identify false assumptions in tests that have led people to eliminate a loading theory. I only list some cases here (11): the element of time in the photoelectric effect, Bothe-Geiger experiment, Compton Simon experiment, photoelectric effect, black body spectrum, oil drop measurement of *e*, and all previous beam-split coincidence tests of the photon model.

A Quantum Mechanical QM particle is generally understood to go one way or another at a beam splitter. They teach that a nucleus or atom is a thing that *somehow* travels as a wave, yet appears as a particle. A particle eliminating the other path at a beam splitter requires nonlocality. I perform beam-split coincidence tests with γ and α-rays, and see coincidence rates far exceeding chance: the unquantum effect.

Here, we interpret our constants h, e, and m (Planck's constant, charge, and mass) as thresholds. Ratios of these constants, like h/m, remain quantized. A matter wave of conserved ratios can thin out, load up to a threshold at an absorber, and give the illusion that a particle crash-landed in guidance by a probability wave.

4) α-split tests with gold (12, 15, 16)

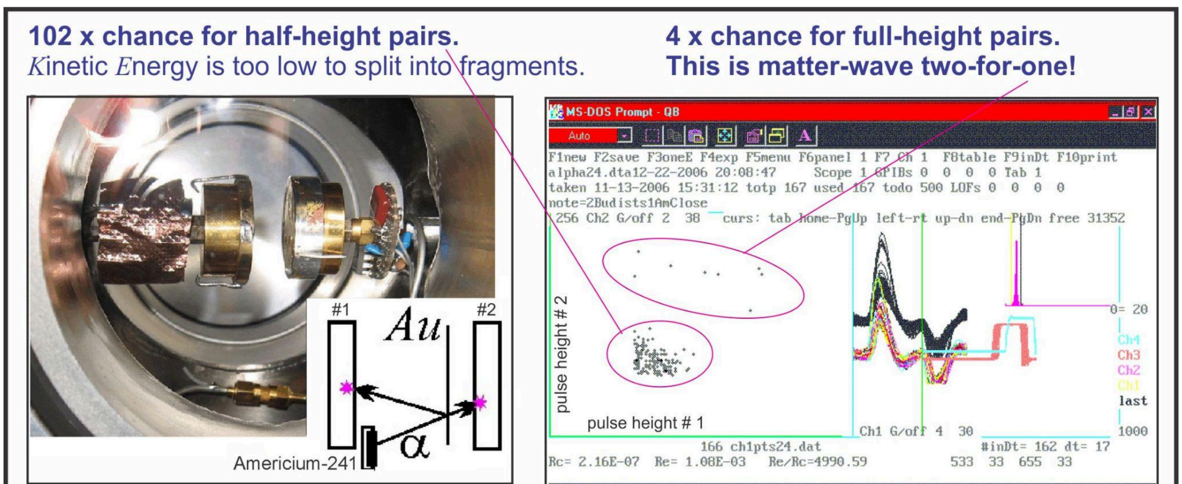

Fig. 5 Automated α-split test of 2006

Fig. 5 shows two surface barrier detectors a cm apart. ^{241}Am emitting 5.5 MeV α was aimed from a side perch toward the right detector, which is covered with gold leaf. This geometry accepts the widest range of interaction angles. The Lecroy scope triggers upon clicks within a preset time window τ to record both pulse heights. The computer plots the pulse heights in an XY graph as shown. Most of the pulses are half height. We calculate a ratio exceeding chance, $R_{experiment}/R_{chance}$, where $R_{chance} = R_1R_2\tau$, and τ = 100 ns. Using the half-height pulses $R_{experiment}/R_{chance}$ = 100. QM predicts chance (ratio = unity), and we call exceeding chance the unquantum effect. Counting the larger pulses exceeds chance by 4. We perform an energy budget based on the characteristic pulse height. When we add the pulse heights of the larger pulse pair, the sum exceeds the characteristic pulse height. The energy budget per pulse pair easily exceeds unity and chance. By a generalized understanding of energy conservation, a pre-loaded energy adds to and is released by a sudden matter wave. The matter reaches a tipping point (threshold). When that threshold is reached, it looks like a particle was absorbed. We are not splitting the α into two deuterons (which requires 14 MeV), nor are we breaking gold nuclei (which requires 26 MeV). We only have 5.5 MeV of kinetic energy. Our measured coincidence background was 1 count over 3 days. All pulses were perfect. A true coincidence test revealed zero *trues*. These tests were on Nov 8-13, 2006.

5) Newly reported α-split tests

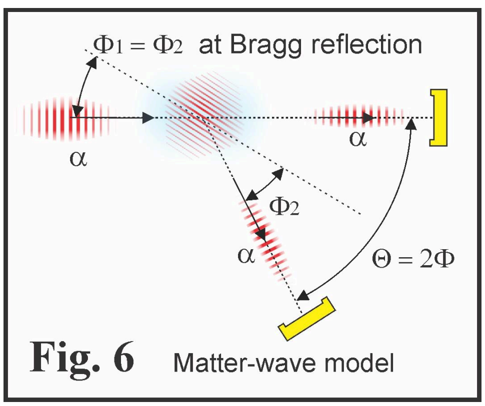

Fig. 6

Fig. 6 outlines how to think about the matter-wave to matter-wave interaction that we provide evidence for. Here, we use a crystalline scatterer, the silicon surface barrier detector. This detector serves a dual purpose: as a detector and as the unquantum beam-splitter. My previous tests of this matter-wave unquantum effect were conducted using gold beam splitters (as above). We adjust the angle of the scatterer and the angle of the deflection detector to test for specular reflection, characteristic of Bragg reflection. The particle model does not predict such a specular effect. Reports of Si crystal α-scattering (13) and specular reflection of atoms from crystals using the de Broglie equation support my model (14). Crystal α scattering and Rutherford backscattering tests by others will calculate the blockage and channeling related to an atomic matrix.

Thirty-eight tests were performed, keeping all variables untouched, except for the angles of our two detectors. **Appendix 2** shows my complete spreadsheet. The detectors, see **Fig. 7**, are ORTEC surface barrier type with an amplifier built in, a discontinued model I was fortunate to find. The ^{241}Am α source is arranged behind the stack of 55 glass pipette tubes.

The crystal beam splitter enhanced the unquantum effect, but obviously, we are not dealing with atomic spacing. We calculate the matter wavelength as usual by $\lambda = h/m_\alpha \boldsymbol{v}$, and substituting for $\boldsymbol{v}$ from kinetic energy = $\mathcal{E} = m\boldsymbol{v}^2/2$. Where $\mathcal{E} = 2*5.5\text{x}10^6$ eV, and $m_\alpha = 3.7\text{x}10^9$ eV/c^2, we obtain $\lambda = 6\text{x}10^{-15}$ m. Using Bragg diffraction at 30°, the distance between resonant reflective planes is

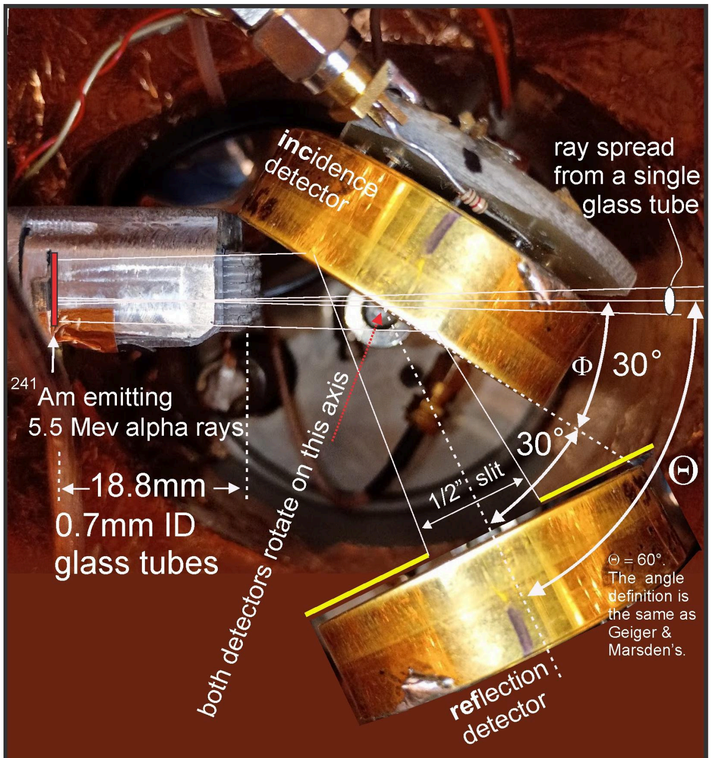

Fig. 7. Experiment at specular 30°.
The image of the reflection detector was pasted in.

3x10^{-15} m. The distance between crystalline *Si* atoms is larger than the α matter-wavelength by 19.5 k. This report shows evidence of α-ray matter-wave interference. To review, the α splits in a *unquantum* sense in its interaction with nuclear-realm silicon. We are examining a matter-wave to matter-wave interaction. Even using the word "nuclear" is a distraction from the intent of this report. We present evidence for an extended, massive, positively charged aspect of the atom with a periodic structure.

Fig. 8 shows selected screen shots from a Lecroy LT624 scope and a custom 4-channel MultiChannel Scaler MCS I wrote in QUICKBASIC for this experiment. All data were obtained from these images. The LT624 triggers upon timing edges from pulse-height discriminators (ORTEC 551) recorded on its channels 3 and 4 that appear within a 2 μs window. Upon a trigger, the LT624 records pulse shapes on traces 1 and 2, both pulse heights to histograms A and B, and histogram C of the time between those two timing edges. The total number of coincident pairs {totp(C)} is counted within a preset 400 ns window τ. {totp(C)}/{dur(C)} deliver the experimental coincidence rate R_e. That same τ is also used for calculating chance, $R_c = R_\Theta R_\Phi \tau$, where we use the same τ. All coincidence data in sections **4**

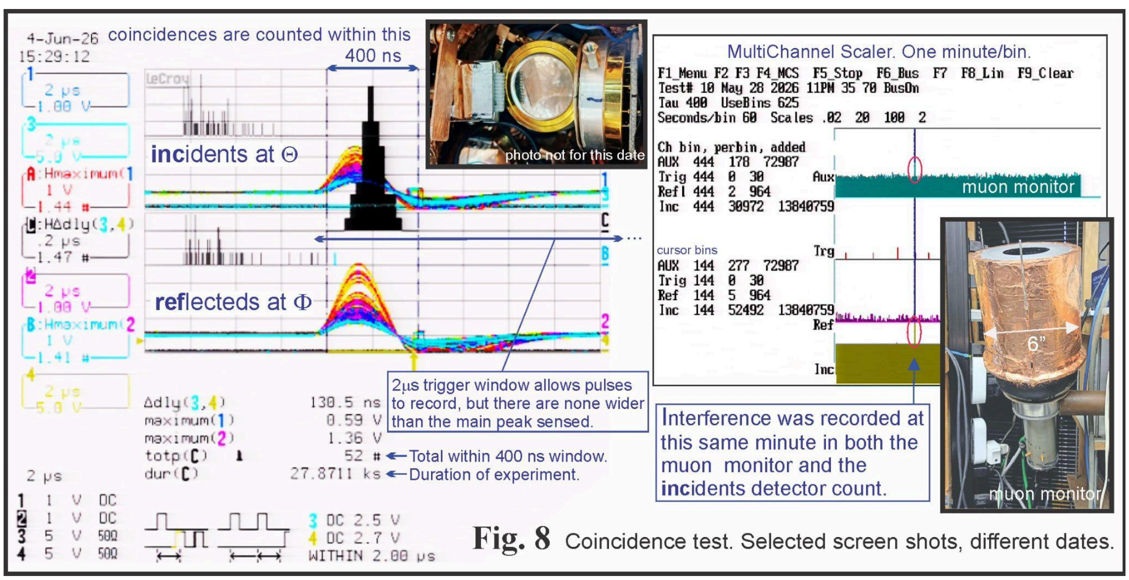

Fig. 8 Coincidence test. Selected screen shots, different dates.

and **5** refute QM. In most cases, τ can be narrowed to calculate R_e/R_c even higher, but we fixed τ to maintain comparison. Notice there are no out-of-time pairs in the wings of C, allowed to span 2 μs. This is far superior to tests with gold splitters.

The MCS records counts each minute from four HP 5334 Universal Counters via GPIB to the PC. Counts accumulated over the entire experiment determine our singles rates R_Φ and R_Θ from the **inc**idents and **ref**lecteds detectors. The MCS also records Lecroy triggers and counts from my muon detector. Due to the low rate of coincidence events, these tests require 5 to 10 hours to read to a few significant figures. During these tests, different forms of interference may occur:

1) Microwave bursts from cell phones can cause wildly shaped pulses on the Lecroy scope, which scrap the test. RF filters were installed, in attempts to remove such disruptions.

2) A background coincidence rate with the source removed measured only 4 in a 48-hour test on June 10, 2026. This is in the spreadsheet calculation.

3) As shown on the MCS, at rare minutes muon counts can nearly double. In that same minute, a similar enhanced count can appear on the record of **inc**idents clicks. Only 3 in 38 recordings have shown this kind of interference. From inspection, these additional **inc** counts can be ignored. An attempt was made to compare against published solar storm and X-ray data, but no conclusion was reached. The parts for this muon detector construction were a giant scintillator plastic and a PMT, of used surplus and unknown specifications.

In **Fig. 9**, we sort our tests to focus on important measures while maintaining the Bragg condition Φ1 = Φ2. The angle Θ orientation of mine and Rutherford is the same, but now with specular crystal reflection arranged with two detectors. From the viewpoint of Rutherford scattering, one might expect the α reflection rate to decline steeply with angle. In these conditions, we see a steep increase with angle. The angle of incidence *by itself* to the gold scatterer made little difference in the singles reflection rate. This enhancement of reflection cannot be explained by inhibited reflection of alphas trapped on the way back, as seen in Rutherford Backscatter Spectroscopy. In RBS, larger angles closer to retroreflection inhibit, not enhance reflection.

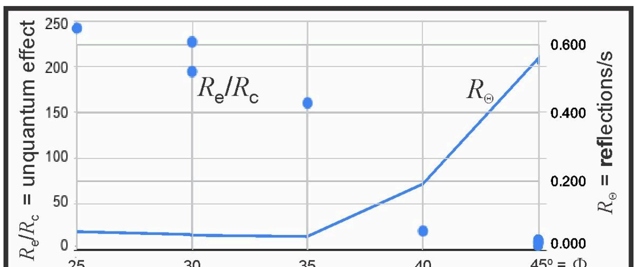

Θ	R_e/R_c	R_Θ = reflections/s
25	242	0.050
30	194	0.042
30	227	0.040
35	160	0.036
40	20	0.190
45	7.3	0.558
45	9.3	0.542

Fig. 9

R_e/R_c and R_Θ.
Both for specular angles
$2\Phi1 = 2\Phi2 = \Theta$

Also in **Fig. 9**, we examine the unquantum effect R_e/R_c at specular angles. In these conditions the unquantum effect is spectacular, near 200 times chance. However, there is a better way to plot to see a trend.

We now make the rate at the scattered angle more important than the ratio above chance (unquantum effect) and look for $R_{\text{coincidence}}/R_{\text{reflecteds}}$ aka R_e/R_Θ as a function of angle-pairs to find which pairs are specular (**Fig. 10**). Discover now, a specular

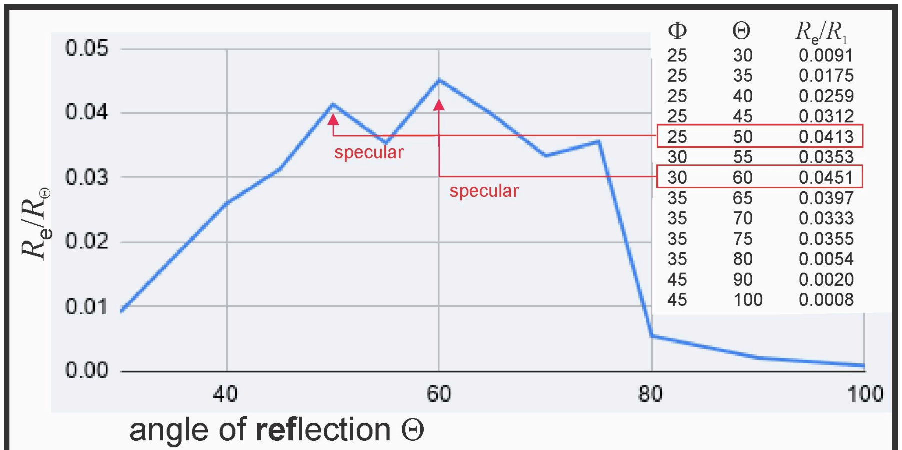

Fig. 10 Plotting only the highest R_e/R_Θ at each Θ

reflection at the two highest points in the graph. This peaks at 2Φ = Θ = 60°, the same angle from X-ray diffraction for silicon (**Fig. 11**). Although we know Bragg distances by X-rays are 20 thousand times larger than by α-rays, we do not ignore this coincidence.

6) Conclusion and speculation

For a different collision phenomenon, the Compton effect, I discovered a beautiful symmetry. A particle derivation and a wave derivation can lead to the same equation (15, 16). Here, we explore physical evidence to illustrate a similar symmetry in matter-matter collisions. A particle- oriented derivation need not prove nature is made of particles.

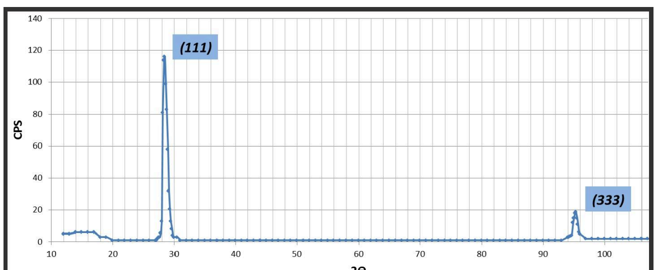

Fig. 11 X-ray analysis of mono-crystalline silicon

Their 2Θ is my Θ. This is the angle between the un-deflected path of the incident beam and the path of the scattered beam traveling toward the detector. Image from https://physicsopenlab.org/2018/01/28/silicon-germanium-crystal-

The unquantum effect is like a filter. Consider that a matter wave can be emitted with arbitrary polarization, similar to the orientation of the electric field of polarized light. Three points define a plane: source, detector 1, detector 2. Hypothesis: when a burst of spontaneously emitted matter-wave has its polarization vector normal to the three-point plane, the wave can undergo a Bragg diffraction split.

According to the particle-nucleus model, the scatterer's surface orientation and its crystalline state should not matter. I make an important note from my older tests. The γ-ray unquantum experiments revealed two effects of the crystalline state: amorphous vs crystalline source, and function of crystal orientation (11). Despite the disparity in scale between alpha matter wavelengths and atomic spacing, the similarity of the X-ray Bragg diffraction angle in silicon in **Fig. 11**, to the peak in **Fig. 10**, suggests a deep, wave-based mechanism of interaction. This jump in scale is suggested in my derivation of the photoelectric effect (11, 15, 16). Light fits a matter-wave envelope composed of an inner, higher-frequency wave. This is the nature of charge. The ratio of inner wave to beat envelope periodicities might explain the jump in scale from atomic to nuclear spatial periodicities we see a hint of here.

My experiments are slow. However, time is something I could take advantage of. Stronger radioisotopes can make my technique practical. Links to spreadsheets and all ER works are at http://www.thresholdmodel.com

References

1. Atom Interferometry, Berman PR, 1996.
2. Towards Realization of an Atomic de Broglie Microscope: Helium Atom Focusing Using Fresnel Zone Plates, Doak RB et al, Phys. Rev. Lett. 83, 4229 (1999). doi.org/10.1103/PhysRevLett.83.4229
3. On the structure of the atom: an investigation of the stability and periods of oscillation of a number of corpuscles arranged at equal intervals around the circumference of a circle; with application of the results to the theory of atomic structure, Thomson JJ, Phil Mag Ser 6. 7:237–265 (1904).
4. The Laws of Deflexion of α Particles Through Large Angles, Geiger H, Marsden E, Phil Mag 25, pages 604–623 (1913).
5. The scattering of α and β particles by matter and the structure of the atom, Rutherford E, Philosophical Magazine, Vol. 21, No. 125, pp. 669–688 (1911).
6. On the constitution of atoms and molecules, Bohr N, Philosophical Magazine, series 6 (1913).
7. Experiments in Modern Physics, Melissinose AC, page 231.
8. A novel design of Rutherford scattering apparatus, Eaton TW, Cheetham D, Phys Educ 8 page 97 (1973).
9. The Atomic Nucleus, Evans RD, Page 18 (1955)
10. Backscatter anomaly in scattering of α-particles from ^{28}Si at low energies, Coban A et al, Nuclear Physics A, 678 pgs 3-10 (2000).
11. Photon violation spectroscopy, Reiter ES, US patent application filed 2005 US20050139776A1 -
12. Particle Violation Spectroscopy, Reiter ES, US patent application filed 2008, US20080173825
13. Backangle anomaly in scattering of alpha-particles from ^{28}Si at low energies, Coban et al, Nuclear Physics A, 678 (2000).
14. The Reflection of Atoms from Crystals, Ellett A, Olson HF, Zahl AH, PR 34, page 493 (1929).
15. New experiments call for a continuous absorption alternative to quantum mechanics-the unquantum effect, Reiter ES, Progress In Physics, vol 2 pg 82 (2014).
16. Overcoming the quantum mechanics measurement problem by experiment and theory, Reiter ES, Physics Essays, Volume 35: Pages 197-201 (2022).

Appendix 1 spreadsheet for June 2026 repeat of 1913 test

A no Au roi = $R_{noAuRoi}$ = background rate in Region Of Interest with gold removed
no Au big = $R_{noAuBig}$ = background rate in big-pulses spectrum with gold removed
no Am roi = $R_{noAmRoi}$ = background rate in ROI spectrum with Americium-241 removed
no Am big = $R_{noAmBig}$ = background rate in big-pulses spectrum with Americium removed
back sums = $R_{backsxx}$ = background rate with Au and ^{241}Am removed. Stated aside for Roi, Big.

B Angle of scatterer detector

C Angle of gold scatterer

D Scale and offset adjustment of angle

E Count **Rate** in **R**egion **O**f **I**nterest spectrum. R_{roi}

F Count **Rate** in **Bigs** spectrum. R_{Bigs}

G $R_{roi} - R_{NoAmRoi} - R_{noAuRoi}$

H $R_{big} - R_{NoAmBig} - R_{noAuBig}$

I Equation developed by Rutherford for rate as function of angle. “1/sin^4”.

J R_{roi}/”sin^4”

K normalization calculation, “1/sin^4”/$R_{roi\ at\ 45°}$.

L Error calculation using ROI data.

M R_{big}/”sin^4”

N normalization calculation, “1/sin^4”/$R_{big\ at\ 45°}$.

O Error calculation using Bigs data.

	A	B	C	D	E	F	G	H	I	J	K	L	M	N	O
1		angle scat det	Gold angle	0.5	Roi	Rbigs	roi minus backs	big minus backs	1/(sinRad(D)^4	roi/sin^4	I/G rescale	roi error I/K	big/sin^4	I/H correction	bigs error
2				0			#	#	1/sin4 theory	G# / theory	90.00005813	should/got	H# / theory	202.986027	should / got
3		45.00	30	22.5	0.47	0.208	0.46726	0.207174	42.05	19.64988438	42.05	1	8.712376719	42.05342716	1
4		60.00	30	30	0.127	0.047	0.12426	0.046174	13.32	1.654801255	11.18	1.190804188	0.6149106162	9.372676812	1.420858568
5		60.00	45	30	0.116	0.039	0.11326	0.038174	13.32	1.508311526	10.19	1.306457075	0.508372631	7.748788596	1.718623239
6		75.00	30	37.5	0.041	0.0141	0.03826	0.013274	5.48	0.2096768229	3.44	1.591540542	0.07274569126	2.694436523	2.033937039
7		90.00	30	45	0.0176	0.004	0.01486	0.003174	2.69	0.04001198611	1.34	2.013305595	0.008546301743	0.6442776498	4.179248874
8	no Au roi	90.00			0.0026										
9	no Au big	90.00				0.005									
10	no Am roi				0.00014										
11	noAm big					0.00326									
12	back sums				0.00274	0.000826									

Appendix 2. Spreadsheet for June 2026 alpha-ray against silicon detector

	Φ angle of **inc**idents detector	Θ angle of **ref**lecteds detector	unquantum effect = R_e/R_c, where R_c = chance = $R_\Theta R_\Phi \tau$	R_e= Experimental coincidence rate within τ winc	R_Θ= reflections/second	R_Φ= incident counts/second	R_e/R_Θ	$1/R_c$ in hours. # of hours to expect a chance coi	Time of experiment recorded on MCS	R_Θ rate of reflection clicks recorded from MCS	R_Φ rate of incident clicks recorded from MCS	time duration of experiment from Lecroy scope	R_e coincidenc counts within τ from Lecroy scop τ = 400 ns.	trigger counts from Lecroy recorded on MCS		# of pulses > 3v from **inc**idents detector.	# triggered pulses outside τ window but in trigger window	# background coincidences, source removed. To be subtracted from R_e
date 2026	**phi**_incidents	**theta**_reflects	***R***e/***R***chance	***R***experiment	***R***theta	***R***phi	***R***e/***R***theta	hours/chance	MCS time	**ref**lecteds	**Inc**idents	DSO secs	DSO coinc	triggers	note	Big **inc**s	out of time DSO	Background 2/day
month/day	**degrees**	**degrees**	**Unquantum**	**coinc/s**	**ref/s**	**inc/s**	**coincs/reflects**	**1/R1*R2*400ns*_**	**seconds**	**# MCS**	**# MCS**	**seconds**	**# in window**	# DSO				#/sec. Use for all
05/22	25	30	52.8	0.00119	0.133	421.760	0.0089	12.342192834564	27000	3602	11387516	25582	31	32		5	0	2.32E-05
05/21	25	35	103.8	0.00183	0.105	421.633	0.0175	15.718865315823	30120	3156	12699577	29449	54	53		many	1	2.32E-05
05/20	25	40	151.6	0.00183	0.071	427.322	0.0259	23.014206375880	37500	2648	16024558	37706	69	68	bigs 32xchance	16	1	2.32E-05
05/20	25	45	185.3	0.00179	0.057	421.556	0.0312	28.734373269787	34380	1971	14493087	34615	62	61	interesting	6	0	2.32E-05
05/19	25	50	241.7	0.00208	0.050	427.309	0.0413	32.212980041858	28860	1456	12332124	28308	59	59	best	6	0	2.32E-05
06/03	25	60	220.4	0.00151	0.040	429.912	0.0379	40.471684194258	18240	728	7841597	16525	25	26		3	1	2.32E-05
05/19	25	65	181.2	0.00126	0.041	427.387	0.0310	39.799004513646	37500	1531	16027015	40326	51	47	dso longer time	2	1	2.32E-05
06/01	25	70	191.1	0.00120	0.037	421.565	0.0322	44.187215156180	37500	1398	15808703	36619	44	41	dso longer time		0	2.32E-05
06/03	25	60	220.4	0.00151	0.040	429.912	0.0379	40.471684194258	18240	728	7841597	16525	25	26		3	1	2.32E-05
06/04	25	55	185.6	0.00137	0.044	422.167	0.0313	37.656217088644	26280	1148	11094549	24840	34	34	peakey	5	0	2.32E-05
06/03	30	40	117.9	0.00168	0.072	495.432	0.0234	19.475315895736	28080	2021	13911722	27345	46	49			3	2.32E-05
05/27	30	55	176.6	0.00154	0.044	499.851	0.0353	31.758544368854	29580	1294	14785601	29140	45	46		5	2	2.32E-05
05/27	30	60	194.3	0.00163	0.042	500.690	0.0389	33.065205635508	37500	1573	18775871	42883	70	58	dso longer time	5	0	2.32E-05
05/23	30	60	226.8	0.00180	0.040	497.201	0.0451	35.004218939800	28320	1130	14080730	26675	48	49			3	2.32E-05
05/27	30	65	163.8	0.00124	0.038	499.968	0.0328	36.805739725614	25200	951	12599187	24264	30	30		4	0	2.32E-05
06/04	30	50	186.0	0.00187	0.051	495.918	0.0369	27.690837877814	28080	1420	13925387	27871	52	52	beauty peak	5	0	2.32E-05
06/05	30	70	166.5	0.00114	0.035	495.245	0.0330	40.545246697637	29580	1023	14649347	25421	29	29	peakey	all both at1/2 hts	0	2.32E-05
05/28	35	55	103.1	0.00111	0.052	519.191	0.0214	25.709702809470	36540	1901	18971227	40403	45	46	bigs 20xchance	9	1	2.32E-05
06/04	35	60	205.2	0.00169	0.040	517.481	0.0425	33.694721237787	26640	1061	13785696	25421	43	44		5	1	2.32E-05
05/28	35	60	157.3	0.00125	0.038	519.139	0.0327	34.820539830987	32460	1247	16851268	31088	39	39		2	1	2.32E-05
06/01	35	65	159.0	0.00124	0.038	518.067	0.0329	35.513324331813	30600	1155	15852839	28946	36	37			2	2.32E-05
05/29	35	65	191.4	0.00143	0.036	518.884	0.0397	37.160331981788	15660	564	8125729	36349	52	28	dso longer time	2	1	2.32E-05
05/29	35	70	160.0	0.00121	0.036	520.329	0.0333	36.826787907611	26600	964	13840759	24860	30	30		2	0	2.32E-05
05/31	35	75	107.9	0.00136	0.060	519.198	0.0224	22.115310901529	37500	2268	19469910	43517	59	34	dso longer time		4	2.32E-05
05/24	35	75	170.9	0.00131	0.037	519.741	0.0355	36.124795110543	37500	1387	19490285	37279	49	48		1	1	2.32E-05
05/31	35	80	25.9	0.00094	0.174	518.557	0.0054	7.694565054519	25080	4365	13005416	23520	22	26			4	2.32E-05
06/04	35	60	206.4	0.00169	0.040	514.478	0.0425	33.891396962904	26640	1061	13705696	25421	43	44		5	1	2.32E-05
06/01	40	50	107.7	0.00106	0.047	526.421	0.0227	28.314134432679	23760	1107	12507758	21762	23	24		3	1	2.32E-05
05/24	40	75	88.3	0.00110	0.059	526.769	0.0186	22.407235354534	27960	1645	14728471	36529	40	40	all in time	0	0	2.32E-05
05/25	40	80	20.4	0.00082	0.190	526.822	0.0043	6.934845439543	37500	7128	19755843	39096	32	35	interesting	4	4	2.32E-05
06/05	40	60	129.0	0.00104	0.038	526.405	0.0272	34.619210396469	25140	958	13233825	22221	23	24		1	1	2.32E-05
06/02	45	45	19.4	0.00017	0.042	530.298	0.0041	31.259876602539	26640	1116	14127148	23223	4	4	maybe shadow		0	2.32E-05
06/02	45	50	55.9	0.00049	0.041	530.411	0.0119	31.846800704371	25200	1036	13366356	22555	11	11		3	0	2.32E-05
06/02	45	90	7.3	0.00086	0.558	530.052	0.0015	2.346159659441	22920	12799	12148793	19676	17	28			11	2.32E-05
05/26	45	90	9.3	0.00107	0.542	530.422	0.0020	2.416503243775	37500	20317	19890838	44018	47	60	dso longer time		many	2.32E-05
06/03	45	100	3.5	0.00082	1.087	538.874	0.0008	1.185799049423	28200	30647	15196258	28111	23	43			10	2.32E-05

Appendix 3. Photo of alpha lab